

PAPER • OPEN ACCESS

Thermal conductivity of SLM deposited H13 steel

To cite this article: K Halmešová *et al* 2021 *IOP Conf. Ser.: Mater. Sci. Eng.* **1178** 012015

View the [article online](#) for updates and enhancements.



ECS **240th ECS Meeting**
Digital Meeting, Oct 10-14, 2021
We are going fully digital!
Attendees register for free!
REGISTER NOW

Thermal conductivity of SLM deposited H13 steel

K Halmešová¹, J Džugan¹, M Ackermann², M Koukolíková¹ and Z Trojanová¹

¹COMTES FHT a.s., Průmyslová 995, 334 41 Dobřany, Czech Republic

²Laboratory of Rapid Prototyping, Centre for Nanomaterials, Advanced Technologies and Innovation, Technical University of Liberec, Studentská 1402/2, 460 01 Liberec 1, Czech Republic

Corresponding author's e-mail address : kristyna.halmesova@comtesfht.cz

Abstract. Hot-worked H13 tool steel was deposited using selective laser melting (SLM) process in different deposition conditions. The samples were deposited in 2 different directions: parallel and perpendicular to the base plate of SLM device. Thermal conductivity of the deposited samples was calculated on the base of laser flash measurements up to 700°C. Furthermore, the thermal expansion, specific heat, and thermal diffusivity of the deposited samples and their variations with different deposition conditions are also presented. To explain the measured differences in thermal properties, some metallographic studies together with porosity investigation are also provided. It was shown that all measured thermal properties of the samples are affected by temperature and that the microstructural defects play an important role for the resulting thermo-physical properties.

1 Introduction

Selective laser melting (SLM) process is one of the complex, most popular, and fastest developing additive manufacturing techniques, where the controlled laser beam scans the selected part of the powder bed and melts the solid material in the form of powder and forms the resulting part adding layer by layer. The production method enables the production of parts with high geometrical requirements that are technically impossible with traditional processing and almost all metals can be processed by SLM [1]. Similar to welding, the residual internal stresses resulting from high temperature gradients, large amounts of thermal expansion, and shrinkage, or nonuniform plastic deformation during the heating and cooling cycles [2] are the major drawbacks of this technique and lead to cracks or distortion of the parts [3,4]. Applying postheat treatment, heating of the substrate plate or rescanning by the laser beam results in the reduction of residual stresses [5].

Another weakness of SLM is the reduced density due to an occurrence of pores, lack of fusion in processed materials. Eventually, these defects act as stress concentration sites that initiate cracks and lead to failure of printed parts [6].

Thermal properties of SLM deposited materials are rarely discussed. H13 tool steel is widely used in the injection moulding industry, especially of aluminum and manganese, because it offers high strength at elevated temperatures, high hardness, and it also has the advantages of high resistance to thermal shock and thermal fatigue, high abrasion resistance and heat resistance. In SLM applications, H13 can also achieve in-situ hardening during SLM manufacture, which can potentially reduce the need for postbuild hardening heat treatment [7]. However, to effectively apply H13 tool steel in SLM manufacture of



injection moulds, it is necessary to carefully manage SLM processing parameters which is discussed in detail in [8].

The thermal properties are interesting especially for hot work tools. Thermal diffusivity is an important transient thermal property, required for such purposes such as design applications, determination of safe operating temperature, process control, and quality assurance [9]. The higher thermal conductivity allows more efficient cooling of the tool and hence shortening of the production time.

In this paper, the specific heat capacity, thermal expansion, density, and thermal diffusivity of SLM prepared H13 specimens were measured and these results were used for the calculation of thermal conductivity. The effect of different deposition parameters on the thermal properties was also studied.

2 Experimental

All samples were manufactured at Technical University of Liberec using SLM280HL machine (SLM Solution AG, Lübeck, Germany). H13 tool steel powder was also provided by the SLM Solutions AG company and the chemical composition (in weight %) is 0.42C, 0.44Mn, 0.85Si, 5.22Cr, 1.50Mo, 1.04V. The laser power for appropriate powder melting was 175 W and the scanning speed was 610 mm/s during the building of the samples. Inner part of the specimen was processed using the stripe hatch strategy. The laser tracks were rotated 90° for each layer to minimize inner porosity. Nitrogen gas was used as a protective atmosphere during the process. The building plate was preheated to 200 °C to minimize the residual stresses in the built samples.

Afterwards, the samples were subjected to heat treatment to remove the internal stresses; annealing at 600 °C for two hours in a protective gas was followed by slow cooling.

All samples were directly manufactured by SLM technique in two different building directions. Only supports were manually removed and no other machining or sample preparations were required. Figure 1 shows the specimen orientation and its designation.

Thermal diffusivity results (a), together with related values of specific heat capacity (c_p) and density (ρ) values, can be used in many cases to derive the thermal conductivity (λ), according to the relationship [9]:

$$\lambda = a c_p \rho. \quad (1)$$

The Laser Flash technique (Linseis LFA 1000) was applied for nondestructive and noncontact determining of the thermal diffusivity and specific heat from room temperature up to 700 °C under vacuum. The integrated motorized sample charger allows measurement of 6 samples at the same time (coin shape with 12.7 mm in diameter and 2 mm in thickness) and the measurement was repeated three times. Then the median, mean, and standard deviation were calculated. The thermal diffusivity value is determined from the specimen thickness and the time required for the rear side to reach 50% of its maximum temperature increase. Pure molybdenum specimen was used as a reference for the specific heat determination based on the comparison method of reference and measured specimen.

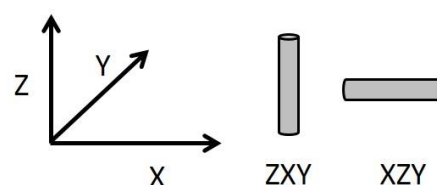


Figure 1: Identification of the dilatometry samples according to the building orientation.

The coefficient of thermal expansion was measured using a dilatometer L75PT (Linseis) up to 1000 °C in an argon protective atmosphere at a cooling/heating rate of 10 °C/min. Correction measurement with Al₂O₃ samples was done to remove the thermal expansion of the instrument. Knowledge of the linear thermal expansion coefficient of the sample dimension (α) and assuming the isotropic behavior, then the sample density relationship over the temperature can be written as:

$$\rho = \rho_{20} / [1 + \alpha(T-20)]^3, \quad (2)$$

where ρ_{20} is the density at the room temperature, which was estimated by the hydrostatic weighting. The microstructure and porosity of the specimens were examined after etching with Villela-Bain chemical agent and using a light microscope NIKON ECLIPSE MA200. Detailed material microstructure was also observed using scanning electron microscope (SEM) JEOL IT 500 HR in the secondary electron regime.

3 Results and discussion

Figure 2a shows the measured dilatometry curves. Phase transformation above 863 °C during heating represents the austenitization of the steel and the transformation during cooling below 310 °C characterized by volume expansion refers to martensitic transformation. Post 700 °C Curie transformation is clearly seen, above this temperature, the relative elongation no longer exhibits a linear character, and therefore the average linear thermal expansion coefficient, α_{20} , between 20 °C and a given temperature, was calculated from the linear part of the dilatometry curve during heating (Figure 2b). Despite the fact that the effect of different building directions seems to be negligible, the thermal expansion is a little lower for sample ZXY at higher temperatures. Using the quasi-harmonic model for atomic vibration, the volumetric thermal expansion coefficient can be described as [10]:

$$\alpha_T^V = \frac{C_{V,T}^V \gamma}{BV}, \quad (3)$$

where α_T^V is the volumetric thermal expansion coefficient, $C_{V,T}^V$ the heat capacity at constant volume, γ the Grüneisen parameter, B the bulk modulus, and V the volume. The lower values of the average linear thermal expansion coefficient for XZY samples may be probably an effect of lower density of the material because of the higher presence of pores (see Figure 4), which originates from unoptimized process parameters. To support this statement, the microstructure of the samples was also provided.

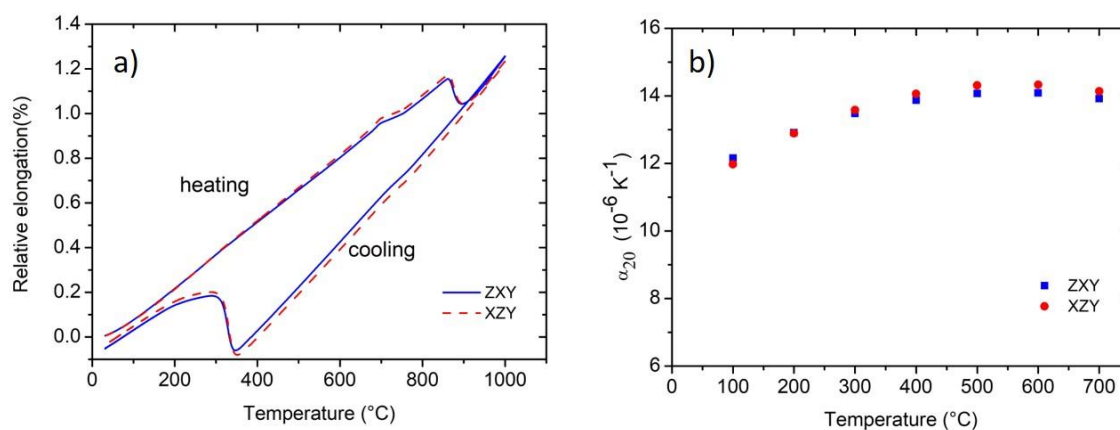


Figure 2: Relative elongation (a) and the average thermal expansion coefficient (b) and their behaviors with the temperature of SLM prepared samples in different directions ZXY and XZY.

Figure 3 shows the microstructure of the samples XZY and ZXY in the plane parallel to the building direction after heat treatment. No important differences in microstructures were observed. Microstructure consists of the tempered martensite with the ferritic matrix and fine carbides. Figure 4 displays the defects in the microstructures (mostly lacks of fusion in our case). It is evident that the specimen ZXY contains a higher fraction of defects. The maximum porosity measured in the worst position in the metallographic sample was 0.02% for XZY and 0.1% for ZXY.

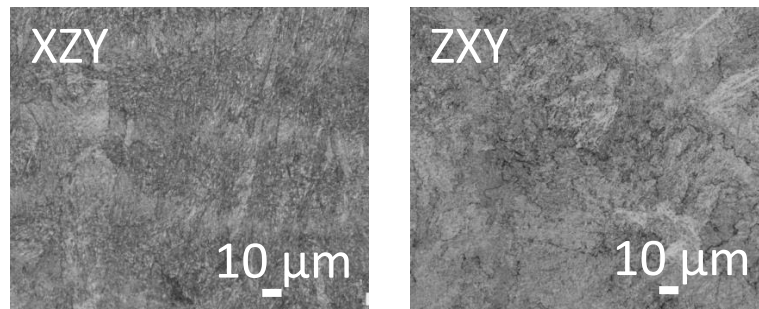


Figure 3: Microstructure of the specimens XZY and ZXY taken from plane parallel to the building direction, after heat treatment.

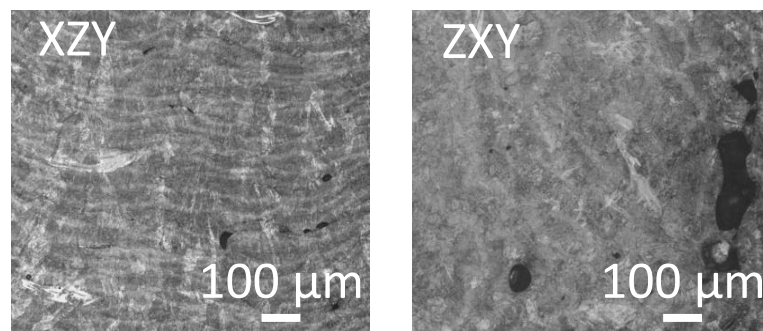


Figure 4: Microstructure defects of the specimens XZY and ZXY taken from plane parallel to the building direction, after heat treatment.

The thermal diffusivity, a , together with the values of the specific heat, c_p , measured from room temperature up to 700 °C are displayed in Figure 5. As seen, the diffusivity values decreased with an increasing temperature for all samples while the specific heat tendency was increasing with rising temperature. These results were used for calculation of the thermal conductivity that is shown in Figure 6.

The thermal conductivity of the material is attributed to the heat transport by electrons and by phonons and can be considered as independent entities. The electron contribution is dominant in pure metals. Even in a concentrated alloy like stainless steel, the electrons carry most of the heat except in the region of the maximum in the phonon part, roughly at $T=0.1\Theta_D$, where the phonons give a significant contribution [11]. For most materials, the Debye temperature is between 200–400 K; Θ_D (Fe) =470 K. The measured thermal conductivity in this work can be described by the electronic contribution to thermal conductivity. Since free electrons are responsible for both electrical and thermal conduction in metals, the two conductivities are related by the Wiedemann-Franz law:

$$\lambda = \sigma LT, \quad (4)$$

where σ is the electrical conductivity and L is a constant (Lorenz number). Therefore, the same factors that affect the electrical conductivity also affect the thermal conductivity. A lower thermal conductivity for ZXY building direction could be caused by higher microstructural defects in the sample as was already mentioned. Ramírez et al. [12] studied the effect of porosity on the thermal properties of aluminum alloy and observed that the thermal conductivity and specific heat capacity decreased with the increase in porosity.

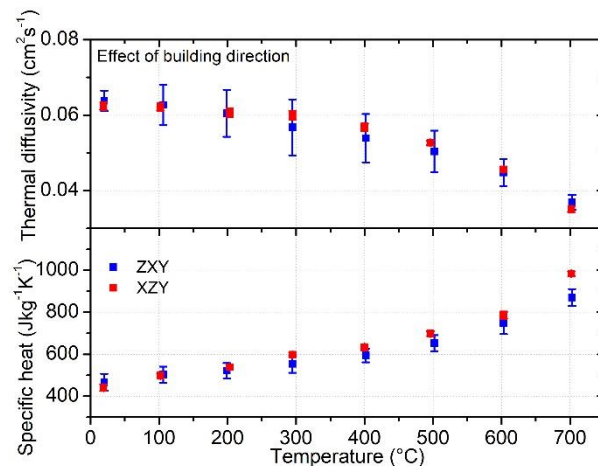


Figure 5: Thermal diffusivity and specific heat as a function of the temperature of SLM prepared samples in different directions ZXY and XZY. The standard deviations are also provided.

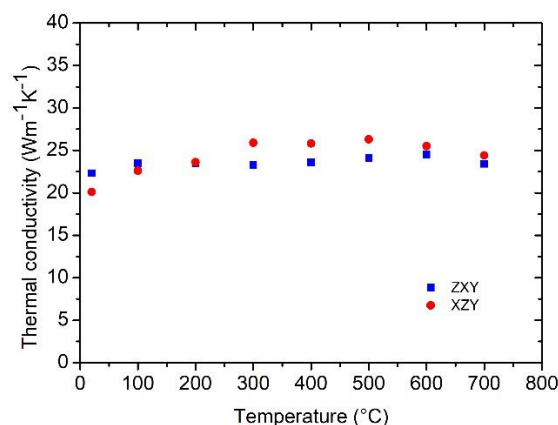


Figure 6: Temperature dependence of the thermal conductivity of SLM prepared samples in different directions ZXY and XZY.

More detailed results of these investigations can be found in [13]

4 Conclusions:

The samples in two different building directions ZXY and XZY were successfully prepared with selective laser melting technology from H13 tool steel powder. Heat treatment afterwards reduced the internal stress and homogenized the microstructure. Microstructure studies proved that there were a lot of microstructural defects resulting from not-well optimized process parameters. The sample ZXY prepared with higher number of layers in z direction suffered from higher concentration of defects compared to the XZY sample. These material imperfections led to lower values of thermal

conductivity, which connects the effect of selective laser melting building direction together with the thermal properties of the printed parts.

Acknowledgement

The paper was supported from the project entitled 3D COVER – Metallic materials in the process chain of additive manufacturing, Project No.: 185, financed by the ERDF.

References

- [1] Kruth J P Mercelis P Vaerenbergh J Froyen L Rombouts 2005 M Binding mechanisms in selective laser sintering and selective laser melting *Rapid Prototyping Journal* **11** pp26-36
- [2] Mercelis P Kruth J P 2006 Residual stresses in selective laser sintering and selective laser melting *Rapid Prototyping Journal* **12** pp254-265
- [3] Yadroitsev I Yadroitsava I 2015 Evaluation of residual stress in stainless steel 316L and Ti6Al4V samples produced by selective laser melting *Virtual and Physical Prototyping* pp67-76
- [4] Kruth J P Deckers J Yasa E Wauthlé R 2012 Assessing and comparing influencing factors of residual stresses in selective laser melting using a novel analysis method, Proceedings of the Institution of Mechanical Engineers, Part B: *Journal of Engineering Manufacture* **226** pp980-991
- [5] Shiomi M Osakada K Nakamura K Yamashita T Abe F 2004 Residual stress within metallic model made by selective laser melting process, *CIRP Annals & Manufacturing Technology* **53** pp195-198
- [6] Brandl E Heckenberger U Holzinger V Buchbinder D 2012 Additive manufactured AlSi10Mg samples using Selective Laser Melting (SLM): microstructure, high cycle fatigue, and fracture behavior *Mater. Des.* pp159-169
- [7] Lee J-H Jang J-H Joo B-D Yim H-S Moon Y-H 2009 Application of direct laser metal tooling for AISI H13 tool steel. *Transactions of Nonferrous Metals Society of China* **19** pp284-287
- [8] Mazur M Leary M McMillan M Elambasseril J Brandt M 2016 SLM additive manufacture of H13 toolsteel with conformal cooling and structural lattices *Rapid Prototyping Journal* Vol. **22** Iss 3 pp504-518
- [9] ASTM E1461-13 2013 Standard Test Method for Thermal Diffusivity by the Flash Method ASTM International, West Conshohocken, PA, www.astm.org
- [10] Zhang X Sun S Xu T 2019 Temperature dependent Grüneisen parameter *Sci. China Technol. Sci.* **62** pp1565-1576
- [11] Grimvall G 1999 Thermophysical properties of materials Elsevier, North Holland Amsterdam ISBN 978-0-444-82794-4
- [12] Ramírez A M Beltrán F J E Yáñez-Limón J M Vorobiev Y V González-Hernández J and Hallen J M 1999 Effects of porosity on the thermal properties of a 380-aluminum alloy *J. Mater. Res.* vol. 14 no. 10 pp3901-3906
- [13] Džugan J, Halmešová K, Ackermann M, Koukolíková M and Trojanová Z 2020 Thermo-physical properties investigation in relation to deposition orientation for SLM deposited H13 steel, *Thermochim. Acta*, **683**(2) 178479